Reactivity and Theoretical Studies of the Unusual Phosphaalkenes *cis/trans*-[$Cp_2(OC)_4Mo_2\{\mu$-η^1:η^2-P(Ph)=C(H)Me$\}$]

Adam J. Bridgeman,[†] Martin J. Mays,*[,‡] and Anthony D. Woods[‡]

Department of Chemistry, University of Hull, U.K., and Department of Chemistry, University of Cambridge, Lensfield Road, Cambridge CB2 1EW, U.K.

Received December 27, 2000

The title complexes provide rare examples of the coordination of a phosphaalkene to a binuclear transition-metal fragment, and the reactivity of these complexes toward a variety of organic and inorganic reagents is reported. A DFT study suggests that the π-bond of the phosphaalkene moiety is essentially lost on coordination, with both the P=C π and π* orbitals being used in bonding to the dimetal core.

Introduction

Phosphaalkenes are currently the subject of intense study,[1−4] the polar nature of the P=C bond meaning that they are ideal precursors to many phosphorus-substituted heterocycles. Phosphaalkene−transition-metal complexes fall into five broad classes (Figure 1); of these type I has attracted by far the most attention. There is surprisingly little literature on the reactivity of phosphaalkenes of types III and V,[2] and even less is known about type IV. To the authors' knowledge there are only two known complexes of type IV in which a phosphaalkene is coordinated to a dinuclear metal fragment as opposed to two mononuclear centers.[5,6]

We recently published a new high-yield synthesis of the dimolybdenum phosphaalkene complexes *cis/trans* [$Cp_2(OC)_4Mo_2\{\mu$-η^1:η^2-P(Ph)=C(H)Me$\}$] (**1**),[6] and herein we present the results of a systematic study of the reactivity of these type IV complexes with metal carbonyls and with organic reagents. It is shown that reaction with metal carbonyls can lead to the formation of mixed-metal tri- and tetranuclear clusters, in which the CHMe part of the phosphaalkene moiety has been eliminated, leaving a phosphinidene capping ligand. The reaction of **1** with organic reagents also leads to breakdown of the phosphaalkene ligand, although complexation of the P=C bond to a metal fragment has clearly made it less susceptible to electrophilic attack.

The results of a DFT study of the isomers *trans*-[$Cp_2(OC)_4Mo_2\{\mu$-η^1:η^2-P(Ph)=C(H)Me$\}$] (**1a)** and *cis*-[$Cp_2(OC)_4Mo_2\{\mu$-η^1:η^2-P(Ph)=C(H)Me$\}$] (**1b)** reveal how best to describe the bonding in complexes of this type and also which of the two isomers of **1** is thermodynamically favored. Unless otherwise stated, however, the reactivity studies reported here utilize a mixture of the *cis* and *trans* isomers of **1**. We have not attempted to study whether the observed reactions are specific to one or the other isomer.

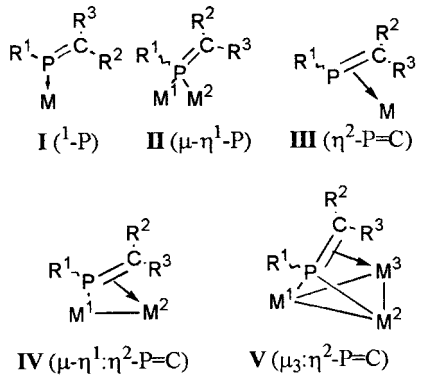

Figure 1. The five types of transition-metal-substituted phosphaalkenes.

Results and Discussion

Protonation. There have been several documented reactions involving protonation of transition-metal-coordinated phosphaalkenes and metallophosphaalkenes. Thus, the protonation of the P atom in [Cp-$(OC)_3$WP=C$(SiMe_3)_2$] in which the phosphorus is σ-bonded to the tungsten was briefly mentioned in a communication,[51] but no X-ray structural data were given for the product. More recently Hill et al. have protonated a series of similarly σ-bonded rutheniophosphaalkenes[7] and Weber has protonated the amino-substituted metallophosphaalkene [$Cp^*(CO)_2$FeP=C-$(NMe_2)_2$].[8] In all these cases the electrophilic addition occurs at the phosphorus atom. However, protonation

* To whom correspondence should be addressed. E-mail: mjm14@cus.cam.ac.uk.
[†] University of Hull.
[‡] University of Cambridge.

(1) Weber, L. *Angew. Chem., Int. Ed. Engl.* **1996**, *35*, 503.
(2) Dillon, K. B.; Mathey, F.; Nixon, J. F. *Phosphorus: The Carbon Copy*; Wiley: New York, 1998.
(3) Yoshifuji, M. *J. Chem. Soc., Dalton Trans.* **1998**, 3343.
(4) Nixon, J. F. *Chem. Rev.* **1988**, *88*, 1327.
(5) Neumann, B.; Schumann, I.; Stammler, H.-G.; Weber, L. *Organometallics* **1995**, *14*, 1626.
(6) Davies, J. E.; Mays, M. J.; Raithby, P. R.; Woods, A. D. *J. Chem. Soc., Chem. Commun.* **1999**, 2455.
(7) Arif, A.; Cowley, A. H.; Dartmann, M. J.; Gudat, D.; Hofmockel, U.; Krebs, B.; Malisch, W.; Niecke, E.; Quashie, S. *J. Chem. Soc., Chem. Commun.* **1985**, 1687.
(8) Bedford, R. B.; Hill, A. F.; Jones, C. *Angew. Chem., Int. Ed. Engl.* **1996**, *35*, 547.

10.1021/om001089k CCC: $20.00
Publication on Web 04/19/2001

Scheme 1. Reaction of 1 with HBF_4

of free phosphaalkenes results in addition to the carbon, as would be expected given the reverse dipole of the P=C fragment.[9] Furthermore, protonation of phosphaalkene−metal complexes in which the metal is datively coordinated by a lone pair on the phosphorus (type I, Figure 1) also results in protonation at the phosphaalkene carbon.[2,10] It thus seemed pertinent to attempt the protonation of **1** to ascertain whether addition of the proton would occur at the phosphorus or carbon centers.

Addition of a slight excess of ethereal HBF_4 to an acetonitrile solution of **1** led to the formation of a red solution. Addition of diethyl ether caused precipitation of red $[\{Cp(MeCN)_4Mo\}_2(\mu\text{-}O)]^{4+}$ (**2**) (Scheme 1), which was then recrystallized by slow evaporation of ether into an acetonitrile solution of **2** to give moderately air stable red crystals in low yield.

The outcome of the reaction in acetonitrile is somewhat surprising. Nixon et al. have reported the stepwise protonation of a coordinated phosphaalkyne to yield an alkylphosphine,[12] and it is proposed that a similar stepwise double protonation of the phosphaalkene occurs to yield a coordinated alkylphosphine in a dicationic intermediate. The displacement of the phosphine and remaining carbonyl groups in **1** by the solvent followed by Mo−Mo bond cleavage would then yield the intermediate $[CpMo(NCMe)_4]^+$. This intermediate is presumably oxidized by adventitious oxygen with concomitant dimerization to give **2**.

Wilkinson et al. reported that protonation of $Mo(CO)_3(NCMe)_3$ always yielded up to 25% $[\{(MeCN)_5Mo\}_2(\mu\text{-}O)]^{4+}$, even under the most rigorous of anaerobic conditions; deliberately allowing air into the reaction vessel gave yields of 90% of the μ-oxo product.[13] It seems likely that a similar mechanism is operative in the current case, with the yields of **2** being noticeably higher if a slight amount of air is allowed into the reaction vessel; reaction of **1** with 4 equiv of HBF_4 in the open air leads to the formation of **2** in near quantitative yield. The sample readily decomposes under vacuum, presumably due to loss of acetonitrile. This decomposition precluded an accurate microanalysis of **2**.

Although molybdenum complexes containing a bridging oxo group are extremely common, all but two of the previously documented complexes also contain terminal Mo=O or Mo=S groups. Of the two complexes which do not, one, $[\{Et_2NCS_2)_3Mo\}_2(\mu\text{-}O)]^+$, is not strictly comparable to **2** because it contains two Mo atoms in different oxidation states.[14] The other example, $[\{(MeCN)_5Mo\}_2(\mu\text{-}O)]^{4+}$, contains a perfectly linear Mo−O−Mo linkage, and the MeCN groups are eclipsed, which suggests a significant dπ−pπ interaction between the Mo and O atoms.[15]

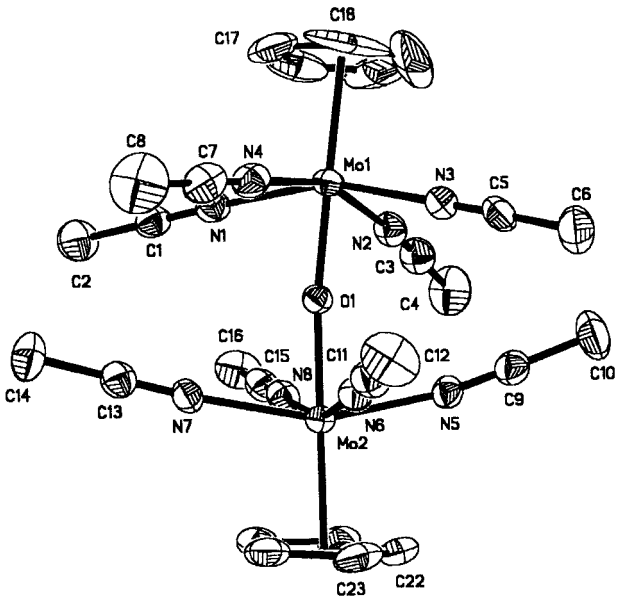

Figure 2. Molecular structure of the cation $[\{Cp(MeCN)_4Mo\}_2(\mu\text{-}O)]^{4+}$ (**2**).

Table 1. Selected Bond Lengths (Å) and Angles (deg) for $[\{Cp(MeCN)_4Mo\}_2(\mu\text{-}O)]^{4+}$ (2)

Mo(1)−O(1)	1.873(2)	Mo(1)−O(1)−Mo(2)	172.2(1)
Mo(1)−N(1)	2.162(3)	O(1)−Mo(1)−N(average)	79.9(2)
Mo(1)−N(2)	2.159(3)	O(1)−Mo(2)−N(average)	79.8(2)
Mo(1)−N(3)	2.161(3)	N(cis)−Mo(1)−N(cis)(average)	88.2
Mo(1)−N(4)	2.158(3)	N(trans)−Mo(1)−N(trans)(average)	159.6
Mo(2)−O(1)	1.889(2)	N(cis)−Mo(2)−N(cis)(average)	88.1
Mo(2)−N(5)	2.136(3)	N(trans)−Mo(2)−N(trans)(average)	159.6
Mo(2)−N(6)	2.157(3)		
Mo(2)−N(7)	2.164(3)		
Mo(2)−N(8)	2.156(3)		

The structure of **2** was confirmed by a single-crystal X-ray diffraction study. The cationic part of the complex is shown in Figure 2, and relevant bond lengths and angles are given in Table 1.

The Mo−O−Mo fragment is not quite linear, with a bond angle of 172.2(1)°, which may be compared to the Mo−O−Mo angles of 175.7° in $[\{Et_2NCS_2)_3Mo\}_2(\mu\text{-}O)]^+$ [14] and of 180° in $[\{(MeCN)_5Mo\}_2(\mu\text{-}O)]^{4+}$.[13] Making the approximation that the Mo−O−Mo fragment is linear allows a calculation of the N−Mo−Mo−N torsion angles; these vary between 40° and 47°, indicating that the MeCN groups are staggered. The Mo−O bonds in **2** [1.873(2) and 1.889(2) Å] are longer than the corresponding bonds in Wilkinson's complex [1.847(3) Å], and are significantly longer than Mo(IV)=O bond lengths (range 1.63−1.69 Å).[16−18] However, the Mo−O−Mo separations are appreciably shorter than Mo−O single bond lengths in other Mo(IV) complexes, and thus some dπ−pπ interaction between the oxygen lone pair and the metal d orbitals seems likely. The staggered arrange-

(9) Laali, K. K.; Neumann, B.; Scheffer, M. H.; Schoeller, W. W.; Stammler, H.-G.; Sundermann, A.; Weber, L. *Organometallics* **1999**, *18*, 4216.
(10) Bickelhaupt, F.; Dam, M. A.; Goede, S. J. *Recl. Trav. Chim. Pays-Bas* **1994**, *113*, 278.
(11) Attali, S.; Caminade, A.-M.; Majoral, J.-P.; Mathieu, R.; Sanchez, M. *Phosphorus Sulfur* **1987**, *30*, 443.
(12) Amélia, M.; Lemos, N. D. A.; Meidini, M. F.; Nixon, J. F.; Pombeiro, A. J. L. *J. Chem. Soc., Dalton Trans.* **1998**, 3319.
(13) Wilkinson, G.; Hursthouse, M. B.; McGilligan, B. S.; Motevalli, M.; Wright, T. C. *J. Chem. Soc., Dalton. Trans.* **1988**, 1737.
(14) Bloomhead, J. A.; Sterns, M.; Young, C. G. *J. Chem. Soc., Chem. Commun.* **1981**, 1262.
(15) Cotton, F. A.; Wilkinson, G. *Advanced Organic Chemistry*; Wiley: New York, 1988; p 466.
(16) Adatia, T.; McPartlin, M.; Mays, M. J.; Morris, M. J.; Raithby, P. R. *J. Chem. Soc., Dalton Trans.* **1989**, 1555.
(17) Alvarez, C.; García, M. E.; Riera, V.; Ruiz, M. A. *Organometallics* **1997**, *16*, 1378.
(18) Haymore, B. L.; Nugent, W. A. *Chem. Rev.* **1980**, *31*, 123.

Scheme 2. Proposed Reaction Pathway Leading to Formation of 3

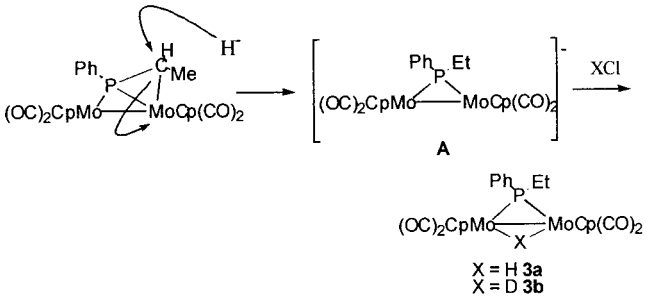

ment of the MeCN groups and the bent Mo−O−Mo bond would suggest that any such dπ−pπ interactions between the filled oxygen p orbitals and the metal d_{xz} and d_{yz} orbitals are not optimal.

The Mo atoms are in slightly distorted octahedral environments, with the equatorial MeCN ligands being tilted toward the axial O site with an average N−Mo−O bond angle of 79.80°. The Mo−N bond lengths vary from 2.157(3) to 2.162(3) Å, these being typical distances for complexes containing acetonitrile ligands coordinated to molybdenum.

Reaction with ^{s}Bu$_3$BHLi. Having studied the reactivity of **1** toward proton sources, it seemed logical to extend the studies to the reactivity of **1** toward hydride sources. Accordingly L-Selectide (L-Selectide = ^{s}Bu$_3$BHLi) was added dropwise to a solution of **1** in THF at −78 °C. A deep purple solution was obtained, the crude infrared spectrum of which was similar to the spectra of many complexes of the type $[Cp_2(CO)_4M_2(\mu\text{-}PR_2)]^-$ (M = Mo or W),[19,20] indicating that an anionic metal complex of this type was present. Addition of 1 equiv of HBF_4 to the anion, followed by filtration through a silica pad and removal of the solvent, led to the isolation of an orange solid, $[Cp_2(CO)_4Mo_2(\mu\text{-}PPhEt)(\mu\text{-}H)]$ (**3a**), in high yield. On the basis of these empirical observations, it is proposed that the initial hydride attack occurs at the phosphaalkene carbon to yield an intermediate metal anion, $[Cp_2(CO)_4Mo_2(\mu\text{-}PPhEt)]^-$ (**A**) (Scheme 2). Huttner and co-workers have similarly reported that reaction of $[(OC)_{10}Fe_3(\mu_3\text{-}\eta^2\text{-}RP{=}CH_2)]$ with H^- results in nucleophilic attack at the phosphaalkene carbon.[21]

To verify this proposed reaction pathway, the reaction was repeated but using DCl instead of HBF_4 as the protonating agent. As before an orange solid was isolated, the ^{31}P NMR spectrum of which clearly shows a 1:1:1 triplet ($^2J_{P-D}$ = 5.6 Hz). Furthermore, the ^{2}H NMR spectrum of this complex consists solely of a doublet at −14.52 ppm, confirming that the product is $[Cp_2(CO)_4Mo_2(\mu\text{-}PPhEt)(\mu\text{-}D)]$ (**3b**) and that the initial attack of the hydride is at the phosphaalkene carbon; no deuteration of the Et group was observed.

The structure of **3a** has been confirmed unambiguously by a single-crystal X-ray diffraction study. The molecular structure of **3a** is presented in Figure 3, and relevant bond lengths and angles are given in Table 2. There are no unusual features in the structure, all bond

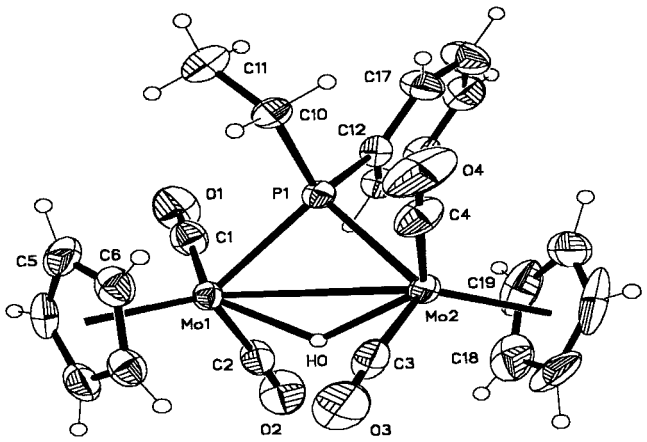

Figure 3. Molecular structure of $[Cp_2(OC)_4Mo_2(\mu\text{-}PPhEt)(\mu\text{-}H)]$ (**3a**) (ORTEP shown to 50% probability).

Table 2. Selected Bond Lengths (Å) and Angles (deg) for 3a

Mo(1)−Mo(2)	3.2775(7)	Mo(1)−Mo(2)−P(1)	47.47(3)
Mo(1)−P(1)	2.425(1)	Mo(1)−Mo(2)−H(0)	27.60(1)
Mo(2)−P(1)	2.434(1)	Mo(1)−P(1)−C(10)	114.9(1)
Mo(1)−H(0)	1.8503(5)	Mo(1)−P(1)−C(12)	122.6(1)
Mo(2)−H(0)	1.8471(5)	Mo(2)−Mo(1)−H(0)	27.55(1)
P(1)−C(10)	1.843(3)	Mo(2)−P(1)−Mo(1)	84.83(3)
P(1)−C(12)	1.832(3)	H(0)−Mo(1)−P(1)	74.48(3)
		H(0)−Mo(2)−P(1)	74.30(3)

lengths and angles being similar to lengths and angles reported for complexes such as $[Cp_2(OC)_4Mo_2(\mu\text{-}PMe_2)(\mu\text{-}H)]$[22] and $[Cp_2(OC)_4Mo_2(\mu\text{-}PPhH)(\mu\text{-}H)]$.[23]

The ^{1}H NMR spectrum of **3a** consists of two very broad singlets in the cyclopentadienyl region. Inspection of the crystal structure clearly indicates that in the solid state these groups are inequivalent, and it is thus apparent that the complex is fluxional in solution but that the process that interconverts the two cyclopentadienyl groups is relatively slow on the NMR time scale at room temperature, hence giving rise to the two very broad resonances. Cooling of the sample to −20 °C leads to a sharpening of the spectrum, giving two very sharp Cp signals. Warming the sample leads to a gradual coalescence of the two signals; thus, at 65 °C a single resonance is observed at 5.02 ppm. The VT ^{1}H NMR spectra of **3a** are shown in Figure 4.

A proposed mechanism for the interconversion of the cyclopentadienyl groups is shown in Scheme 3. The two isomers both possess a square pyramidal geometry, and are interconverted via an intermediate which has a trigonal bipyramidal geometry (ignoring the metal−metal bond in all cases). Such a mechanism has been previously proposed to explain the fluxionality of $[Cp_2(OC)_4Mo_2(\mu\text{-}PPhH)(\mu\text{-}H)]$[23] and $[Cp(OC)_6MoFe(\mu\text{-}AsMe_2)]$[24] as well as of several heterodinuclear manganese−molybdenum complexes.[25]

Reaction with Phosphines. It was hypothesized that addition of a two-electron donor to **1** might displace the η^2-coordination of the phosphaalkene. Thus, **1** was separately reacted with Ph_2PH, Ph_3P, and $(MeO)_3P$. Prolonged thermolysis of **1** with Ph_2PH led to a signifi-

(19) Davies, J. E.; Mays, M. J.; Raithby, P. R.; Shields, G. P.; Tompkin, P. K. *J. Chem. Soc., Dalton Trans.* **1997**, 361.
(20) Davies, J. E.; Feeder, N.; Gray, C.A.; Mays, M. J.; Woods, A. D. *J. Chem. Soc., Dalton Trans.* **2000**, 1695.
(21) Brauer, D. J.; Ciccu, A.; Fischer, J.; Hessler, G.; Stelzer, O.; Sheldrick, W. S. *J. Organomet. Chem.* **1993**, *462*, 111.
(22) Peterson, J. L.; Stewart, R. P. *Inorg. Chem.* **1980**, *19*, 186.
(23) Henrick, K.; Horton, A.; McPartlin, M.; Mays, M. J. *J. Chem. Soc., Dalton Trans.* **1988**, 1083.
(24) Bullock, R. M.; Casey, C. P. *J. Organomet. Chem.* **1981**, *218*, C47.
(25) Bullock, R. M.; Casey, C. P. *Organometallics* **1984**, *3*, 1100.

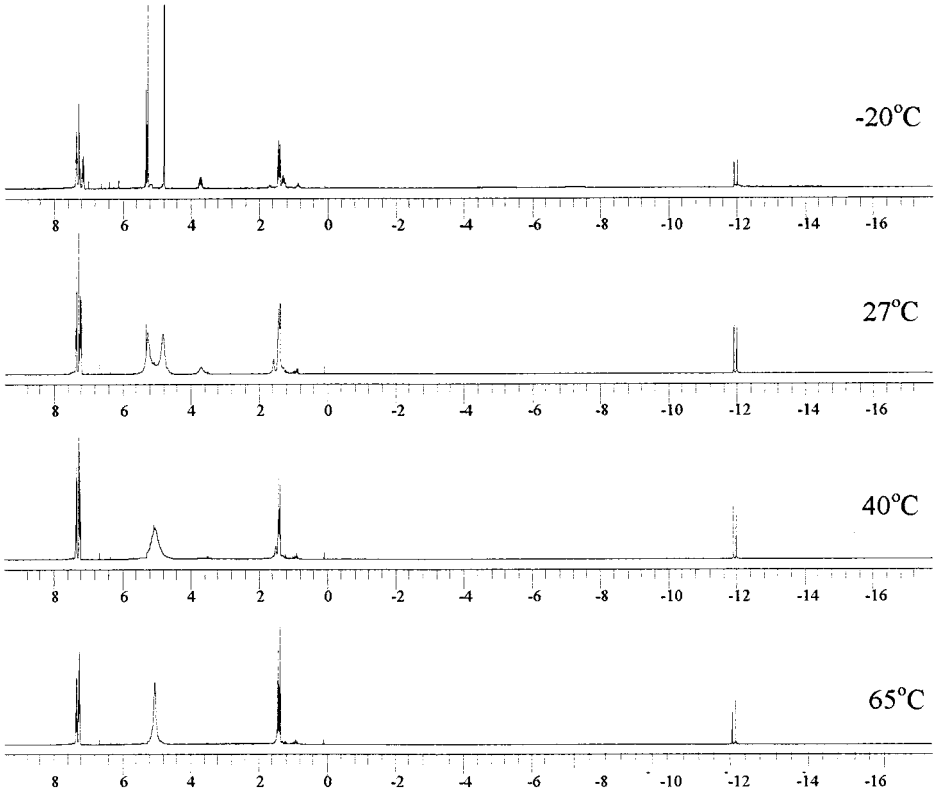

Figure 4. VT ^{1}H NMR spectra of $[Cp_2(OC)_4Mo_2(\mu\text{-}PPhEt)(\mu\text{-}H)]$ (**3a**).

Scheme 3. Proposed Pathway Leading to Fluxionality of 3

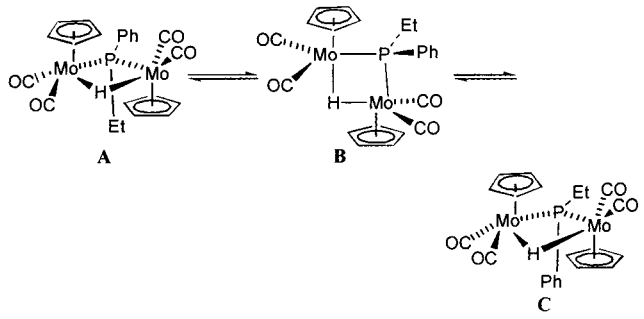

cant amount of decomposition together with the formation of a new red complex in very low yield, which initially was not fully characterized.

In contrast, photolysis of a toluene solution of **1** with Ph_2PH yielded green $[Cp_2(OC)_2Mo_2(\mu\text{-}PPh_2)(\mu\text{-}PPhEt)]$ (**4**) in 63% yield. Consideration of this result led to the realization that the low-yield red product formed on thermolysis was oxidized **4**, $[Cp_2(OC)(O)Mo_2(\mu\text{-}PPh_2)(\mu\text{-}PPhEt)]$, which exists as a chromatographically inseparable mixture of the *trans*-**5** and *cis*-**6** isomers. The oxidation of complexes analogous to **4** is well documented,[26,27] and the hypothesis that in the thermolysis reaction **5** and **6** are derived from **4** was tested by stirring a small portion of **4** in dichloromethane. This led to the formation of **5** and **6** in moderate (40%) yield. Integration of the ^{1}H NMR spectra suggests that the isomers are present in a 4:1 ratio.

A possible course for the reaction leading to **4**−**6** is shown below (Scheme 4). The diphenylphosphine is

Scheme 4. Proposed Reaction Pathway Leading to Formation of 4

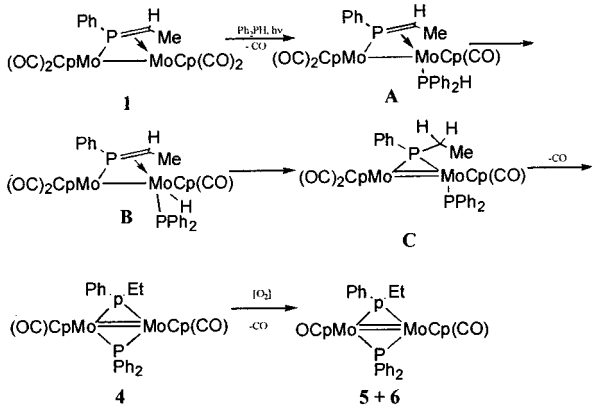

assumed to substitute a CO group in **1**, yielding intermediate **A**. It is proposed that oxidative addition of the datively bound Ph_2PH group then occurs, yielding **B**, this being followed by reductive elimination to give the 16-electron intermediate **C**. Finally, the pendant phosphide group can coordinate to the second molybdenum atom, with concomitant CO elimination and formation of a metal−metal double bond to give **4**.

Similar routes have been proposed to explain the formation of $[Cp(OC)_3MoCo\{\mu\text{-}C(CO_2Me)=C(H)CO_2Me\}(\mu\text{-}PPh_2)]$ in the cothermolysis of $[Cp(OC)_5MoCo(\mu\text{-}\eta^2\text{-}DMAD)]$[28] and Ph_2PH and to explain the formation of $[Cp_2(OC)_2Mo_2\{\mu\text{-}\eta^3\text{-}CH=CHC(O)H\}(\mu\text{-}PPh_2)]$ from $[Cp_2(OC)_4Mo_2(\mu\text{-}HC\equiv CH)]$ and Ph_2PH.[29] Interestingly, in

(26) Adatia, T.; McPartlin, M.; Mays, M. J.; Morris, M. J.; Raithby, P. R. *J. Chem. Soc., Dalton Trans.* **1989**, 1555.
(27) Alvarez, C.; García, M. E.; Riera, V.; Ruiz, M. A. *Organometallics* **1997**, *16*, 1378.
(28) Martín, A.; Mays, M. J.; Raithby, P. R.; Solan, G. A. *J. Chem. Soc., Dalton Trans.* **1993**, 1431.
(29) Doel, G. R.; Feasey, N. D.; Knox, S. A. R.; Orpen, A. G.; Webster, J. *J. Chem. Soc., Chem. Commun.* **1986**, 542.

Scheme 5. Possible Reaction Pathways Leading to Formation of 7

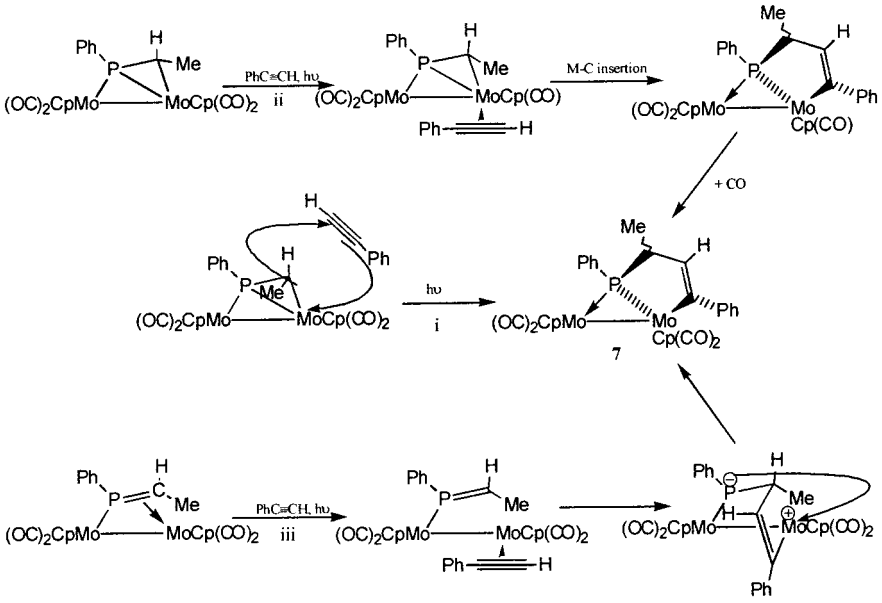

the latter reaction Knox reported that the product was a result of thermolysis, whereas photolysis resulted in the simple substitution of a CO group by the phosphine.

The ^{31}P NMR spectrum of **4** consists of two doublets at 89.10 ppm ($^2J_{P-P}$ = 8.8 Hz) and 84.92 ppm ($^2J_{P-P}$ = 8.8 Hz) which are assigned to the μ-PPh_2 and μ-PPhEt groups, respectively. Oxidation of **4** to yield **5** and **6** causes a downfield shift of the phosphorus resonances, such downfield shifts on oxidation being commonly reported; the assignments of the individual resonances to **5** or **6** are based on a comparison of the $^2J_{P-P}$ coupling constants with literature values for similar compounds[26,27]

The ^{1}H NMR spectrum of the mixture of **5** and **6** consists of multiplet resonances between 8.2 and 7.05 ppm, assigned to the phenyl protons. Four distinct cyclopentadienyl resonances are observed at 5.24, 4.98, 4.82, and 4.80 ppm, the first two resonances being assigned to the cyclopentadienyl groups of **6** and the second two to the cyclopentadienyl groups of **5** by comparison with the spectra of other complexes of this type.

Attempts to react **1** with Ph_3P or $(MeO)_3P$ resulted in the formation of a dark green solution. However, it was not possible to separate the products by conventional chromatographic methods or to identify any of them.

Reaction with Phenylacetylene. Reaction of uncoordinated phosphaalkenes with alkynes leads to cyclization, and the formation of a wide range of products.[1,30] It thus seemed of interest to pursue the reactivity of **1** toward alkynes, phenylacetylene being chosen as a representative example.

Photolysis of a toluene solution of **1** with an excess of HC≡CPh using a 400 W UV lamp for 1 h led to the formation of a purple solution. Separation by TLC led to the isolation of the orange, crystalline insertion product $[Cp_2(OC)_4Mo_2\{\mu$-PhPC(Me)HC(Ph)=CH$\}]$ (**7**) (Scheme 5) as a mixture of isomers.

Insertion of unsaturated hydrocarbons into metal−carbon bonds is common,[31−33] although it is relatively rare to find such reactions taking place at dimolybdenum centers; the reaction reported here is also somewhat unusual inasmuch as no carbonyl ligands have been substituted. In the vast majority of such alkyne insertion reactions the proposed mechanism involves the substitution of a carbonyl ligand by the incoming alkyne followed by carbon−carbon bond formation, or by direct alkyne coupling without ligand displacement.[34,35]

There are several examples in the literature of the coupling of alkynes and metallophosphaalkenes to give metalloheterocycles, although it must be stressed that in these cases neither the alkyne nor the P=C double bond is coordinated to the metal prior to the coupling.[1] Cyclization reactions similar to those reported here for a dinuclear phosphaalkene complex have been reported previously for dinuclear phosphaalkyne complexes, and these latter reactions yield a wide variety of metal-coordinated phosphorus heterocycles.[36−38]

For the reaction reported here three pathways can be proposed (Scheme 5). The reaction could occur via a [2+2] cycloaddition of the alkyne to the Mo−C bond (route i). Alternatively, the phenylacetylene could substitute a carbonyl group and insert into the Mo−C bond (route ii); this would yield a 34-electron intermediate which could then add CO. The reaction was performed with a N_2 purge, so it is unlikely that any of the

(30) Mathey, F.; Marinetti, A.; Bauer, S.; Le Floch, P. *Pure Appl. Chem*. **1991**, *63*, 855.

(31) Ilg, K.; Werner, H. *Organometallics* **1999**, *18*, 5426 and references therein.

(32) Otsuka, S.; Nakamura, A. *Adv. Organomet. Chem*. **1976**, *14*, 251.

(33) Templeton, J. L. *Adv. Organomet. Chem*. **1989**, *29*, 83.

(34) Whitely, M. W. In *Comprehensive Organometallic Chemistry*; Abel, W. E., Stone, F. G. A., Wilkinson, G., Eds.; 1995; Vol. 5, Chapter 6.2.

(35) Chisholm, M. H.; Hoffman, D. M.; Huffman, J. C. *J. Am. Chem. Soc.* **1984**, *106*, 6806.

(36) Leininger, S.; Nachbauer, A.; Peters, C.; Preuss, F.; Regitz, M.; Tabellion, F. *Angew. Chem., Int. Ed. Engl.* **1998**, *37*, 1233.

(37) Johnson, B. F. G.; Nixon, J. F.; Nowotny, M.; Parsons, S. *J. Chem. Soc., Chem. Commun*. **1998**, 2223.

(38) Dickson, R. S.; Francis, M. D.; Hibbs, D. E.; Hursthouse, M. B.; Jones, C.; Junk, P. C.; Richards, A. F. *Organometallics* **1999**, *18*, 4838.

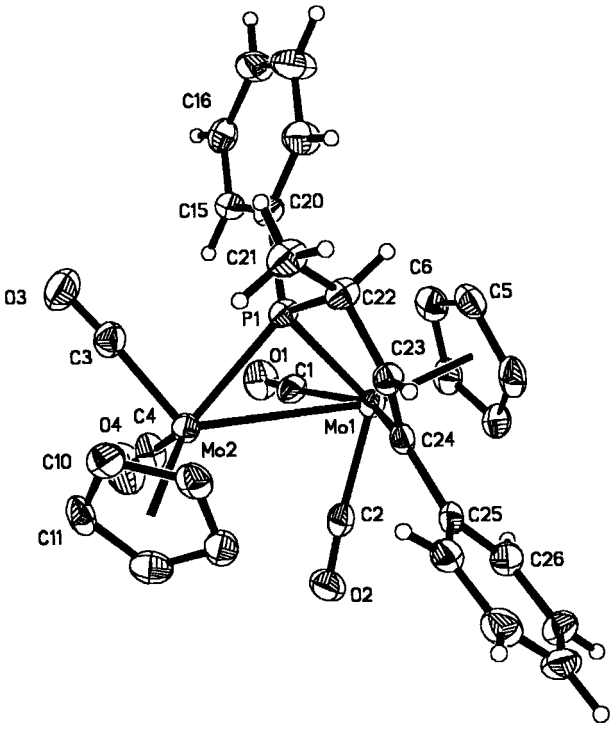

Figure 5. Molecular structure of $[Cp_2(OC)_4Mo_2\{\mu$-PhPC(Me)HC(Ph)=CH$\}]$ (**7**).

Table 3. Selected Bond Lengths (Å) and Angles (deg) for 7

Mo(1)−Mo(2)	3.2309(6)	Mo(1)−P(1)−Mo(2)	83.66(2)
Mo(1)−P(1)	2.424(1)	Mo(1)−C(1)−O(1)	167.9(4)
Mo(1)−C(24)	2.303(5)	Mo(1)−C(24)−C(23)	118.1(3)
Mo(2)−P(1)	2.421(1)	Mo(1)−C(24)−C(25)	124.8(3)
C(24)−C(23)	1.347(7)	Mo(2)−Mo(1)−C(24)	78.5(1)
C(23)−C(22)	1.496(6)	P(1)−C(22)−C(23)	104.3(3)
		C(23)−C(24)−C(25)	116.3(4)

substituted CO groups would remain in solution, but CO groups could be scavenged from decomposition products formed during the reaction. The modest (50%) yield would make such a process conceivable. If such a pathway were followed, then one would expect the yield to be appreciably higher if the reaction were carried out under a CO atmosphere, which was not the case.

Finally, a third possible pathway (route iii) involves displacement of the phosphaalkene from coordination to the second metal center on the approach of the alkyne, resulting in a vacant coordination site. Once coordinated, the alkyne could then add to the phosphaalkene moiety, ultimately leading to the formation of **7**.

To characterize **7** unambiguously, a single-crystal X-ray diffraction study was undertaken. The molecular structure is shown in Figure 5, and relevant bond lengths (Å) and angles (deg) are presented in Table 3. Several complexes with similar structures, but containing a bridging carbene rather than a phosphido group, have been previously formed by insertion of alkynes into Mo−H[39] or Mo=C bonds, and these serve as useful structural comparisons.[40,41] The Mo(1)−C(24) bond length of 2.303(5) Å in **7** is somewhat longer than the values recorded for other complexes containing a molybdacyclopentene moiety.[39−41]

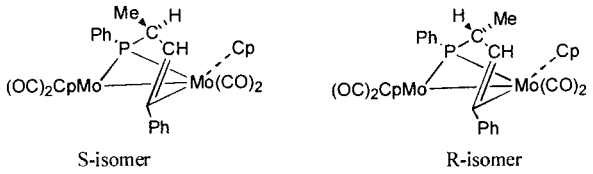

Figure 6. Two possible isomers of **7**.

The C(24)−C(23) bond separation of 1.347(3) Å is typical of an uncoordinated C=C double bond but is somewhat shorter than the value recorded for other molybdacyclopentenes, in which the alkene is η^2-coordinated to the second metal center.[40,41] The bond angles about C(24) reveal a slight distortion from idealized sp^2 hybridization, with the Mo(1)−C(24)−C(25) angle being 124.8(3)° rather than 120°, presumably to relieve steric clashes between the $MoCp(CO)_2$ fragment and the phenyl group. As a consequence the C(23)−C(24)−C(25) and Mo(1)−C(24)−C(23) bond angles are narrowed somewhat to 116.3(4)° and 118.1(3)°, respectively. The phosphido group bridges the two molybdenum atoms symmetrically within experimental error [P(1)−Mo(1) 2.424(1) Å, P(1)−Mo(2) 2.421(1) Å], these separations being typical values for these bonds. The Mo(1)−C(1)−O(1) bond angle of 167.9(4)° suggests some semibridging character, although the Mo(2)−C(1) separation of 3.193 Å is somewhat long for such an interaction.

There are several possible isomers of **7**, two of which are observed in the solution NMR spectra. It seems most likely that the two isomers are derived from the *cis* and *trans* isomers of **1**; these would give rise to *R* and *S* isomers of **7** in the step involving addition of the alkyne to the phosphaalkene carbon (Figure 6). The crystal structure is that of the isomer having an *S* configuration about C22.

Two double doublets can clearly be seen in the ^1H NMR spectrum of **7** at 1.64 ppm ($^3J_{P-H}$ = 15.65 Hz, $^3J_{H-H}$ = 7.83 Hz) and at 1.05 ppm ($^3J_{P-H}$ = 13.69 Hz, $^3J_{H-H}$ = 6.85 Hz), which are assigned to the methyl group of the *S* and *R* isomers, respectively. Two broad multiplets at 3.90 and 3.60 ppm are assigned to the P−C*H* group. Theoretically the resonances due to this group should each be split into a quartet of double doublets, but resolution was poor and the individual coupling constants could not be fully resolved. Two cyclopentadienyl resonances at 5.13 and 4.88 ppm are assigned to the inequivalent Cp groups of the *S* isomer, and two at 5.30 and 4.98 ppm to those of the *R* isomer. A double doublet resonating at 5.86 ppm ($^3J_{P-H}$ = 43.04 Hz, $^3J_{H-H}$ = 3.91 Hz) is assigned to the C=CH group of the *S* isomer. The corresponding resonance of the *R* isomer is significantly broader, and the $^3J_{H-H}$ coupling could not be resolved. The peak is centered at 5.88 ppm with $^3J_{P-H}$ = 36.19 Hz. The ^{31}P NMR spectrum of **7** consists of a very broad peak at 226 ppm, which is presumably due to the overlapping resonances of the two isomers.

Reaction with Metal Carbonyls. Thermolysis of a toluene solution of **1** with $M_3(CO)_{12}$ followed by TLC led

(39) Horton, A. D.; Mays, M. J.; Raithby, P. R. *J. Chem. Soc., Chem. Commun.* **1985**, 247.
(40) Garcia, M. E.; Jeffrey, J. C.; Sherwood, P.; Stone, F. G. A. *J. Chem. Soc., Dalton Trans.* **1988**, 2443.
(41) Adams, H.; Gill, L. J.; Morris, M. J. *J. Chem. Soc., Dalton Trans.* **1998**, 2451.

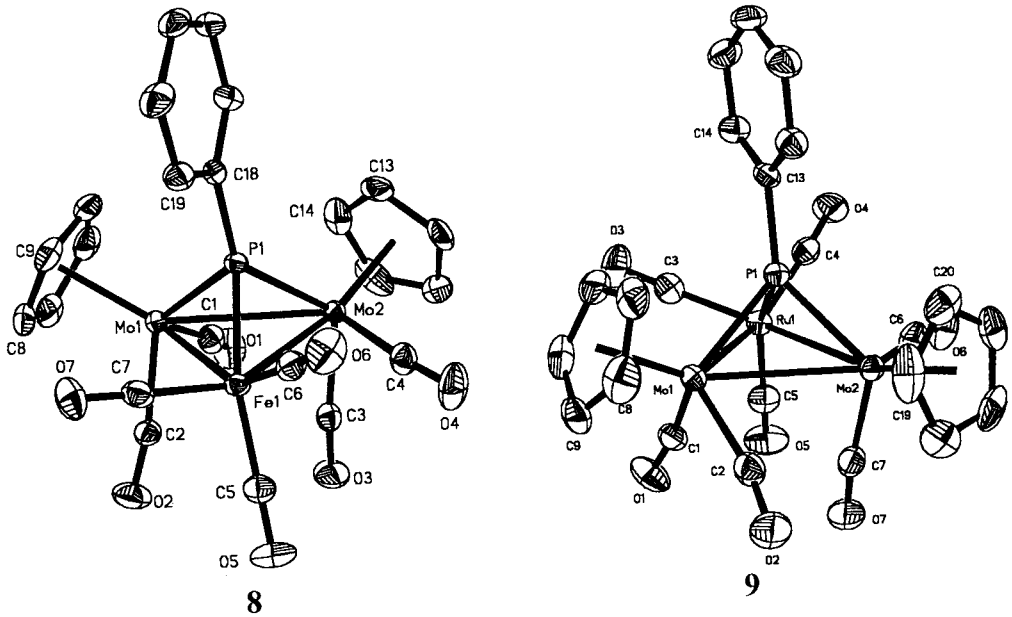

Figure 7. Molecular structures of $[Cp_2(OC)_7Mo_2M(\mu_3\text{-PPh})]$, M = Fe (**8**), M = Ru (**9**) (hydrogen atoms omitted for clarity, ORTEPs at 50% probability).

Scheme 6. Reaction of 1 with Metal Carbonyls

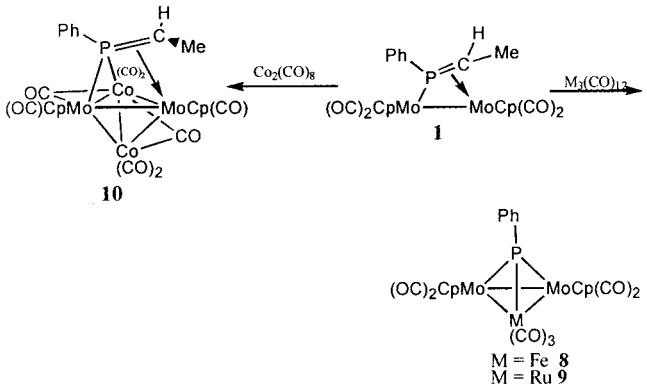

to the isolation of $[Cp_2(OC)_7Mo_2M(\mu_3\text{-PPh})]$ (M = Fe (**8**), Ru (**9**)) each in ca. 35% yield (Scheme 6). It was found that higher yields of **8** were obtained if a solution of **1** was photolyzed with $Fe(CO)_5$. Due to the difficulties in preparing $Ru(CO)_5$ this method was not employed for the preparation of **9**.

Thermolysis of a toluene solution of **1** with $Co_2(CO)_8$ led to the formation of a different type of product, $[Cp_2(OC)_6Mo_2Co_2(\mu\text{-CO})_2\{\mu_3\text{-P(Ph)=C(H)Me}\}]$ (**10**) in 10% yield (Scheme 6). It was found that $[(OC)_6Co_4(\mu\text{-CO})_3(\eta^6\text{-PhMe})]$ was also formed in 30% yield. Complexes of this latter type are well documented, being formed from prolonged thermolysis of $Co_2(CO)_8$ in aromatic solvents.[42] It was found that yields of **10** were increased by thermolysis of **1** with $Co_2(CO)_8$ in nonaromatic solvents such as heptane under a CO atmosphere, although yields were never better than 20%.

Reaction of **1** with other metal carbonyls such as $Mn_2(CO)_{10}$, $W(CO)_6$, and $[Cp_2(OC)_2Fe_2(\mu\text{-CO})_2]$ resulted only in decomposition.

Complexes **8**−**10** have been characterized by FAB MS, microanalysis, and IR, ^1H NMR, and ^{31}P NMR spectroscopy. Additionally, each complex has been the subject of a single-crystal X-ray diffraction study.

Table 4. Selected Bond Lengths (Å) and Angles (deg) for 8 and 9

8		9	
Mo(1)−Fe(1)	2.8949(4)	Mo(1)−Mo(2)	3.1725(8)
Mo(1)−Mo(2)	3.1613(2)	Mo(1)−Ru(1)	2.9687(8)
Mo(1)−P(1)	2.3706(6)	Mo(1)−P(1)	2.378(1)
Mo(2)−Fe(1)	2.9217(4)	Mo(2)−Ru(1)	2.9958(8)
Mo(2)−P(1)	2.3544(6)	Mo(2)−P(1)	2.371(1)
Fe(1)−P(1)	2.1461(7)	Ru(1)−P(10)	2.260(1)
Mo(1)−Fe(1)−Mo(2)	65.84(1)	Mo(1)−Ru(1)−Mo(2)	64.26(2)
Mo(1)−Fe(1)−P(1)	53.64(2)	Mo(1)−Ru(1)−P(1)	51.99(2)
Mo(1)−Mo(2)−Fe(1)	56.67(1)	Mo(1)−Mo(2)−Ru(1)	57.45(2)
Mo(1)−Mo(2)−P(1)	48.23(2)	Mo(1)−Mo(2)−P(1)	48.19(3)
Mo(1)−P(1)−C(18)	127.02(7)	Mo(1)−P(1)−Mo(2)	83.81(4)
Mo(1)−C(1)−O(1)	167.6(2)	Mo(1)−P(1)−Ru(1)	79.55(3)
Mo(1)−C(2)−O(2)	168.3(2)	Mo(1)−P(1)−C(13)	128.0(1)
Mo(1)−P(1)−Mo(2)	83.99(2)	Mo(1)−C(1)−O(1)	166.5(3)
Mo(1)−P(1)−Fe(1)	79.55(2)	Mo(1)−C(2)−O(2)	170.9(3)
Mo(2)−Fe(1)−P(1)	52.70(2)	Mo(2)−Mo(1)−Ru(1)	58.28(2)
Mo(2)−Mo(1)−Fe(1)	57.49(1)	Mo(2)−Mo(1)−P(1)	48.00(3)
Mo(2)−Mo(1)−P(1)	47.79(2)	Mo(2)−Ru(1)−P(1)	51.34(2)
Mo(2)−P(1)−Fe(1)	80.82(3)	Mo(2)−P(1)−Ru(1)	80.48(3)
Mo(2)−P(1)−C(18)	138.16(7)	Mo(2)−P(1)−C(13)	137.3(1)
Mo(2)−C(4)−O(4)	171.8(2)	Mo(2)−C(6)−O(6)	170.9(3)
Fe(1)−Mo(1)−P(1)	46.81(2)	Ru(1)−Mo(1)−P(1)	48.46(3)
Fe(1)−Mo(2)−P(1)	46.48(2)	Ru(1)−Mo(2)−P(1)	48.08(3)
Fe(1)−P(1)−C(18)	127.17(7)	Ru(1)−P(1)−C(13)	127.4(1)

The molecular structures of **8** and **9** are shown in Figure 7, and relevant bond lengths (Å) and angles (deg) are given in Table 4. The Mo_2Fe core present in **8** is somewhat different from that in the related complex $[Cp_2(OC)_7Mo_2Fe\{\mu_3\text{-PMoCp(CO)}_3\}]$,[43] having significantly longer bond lengths within the triangular core [Mo(1)−Fe(1) 2.8949(4) Å, Mo(2)−Fe(1) 2.9217(4) Å, Mo(1)−Mo(2) 3.1613(2) Å]. As is to be expected the phosphorus atom caps the triangle asymmetrically with a short Fe−P separation of 2.1461(7) Å, and somewhat longer Mo−P separations [Mo(1)−P 2.3706(6) Å, Mo(2)−P 2.3544(6) Å]. All of these distances are significantly shorter than the corresponding distances in $[Cp_2(OC)_7Mo_2Fe\{\mu_3\text{-PMoCp(CO)}_3\}]$, presumably because the P−*Ph* group is significantly smaller than the P−*MoCp(CO)*$_3$

(42) Bird, P. H.; Fraser, A. R. *J. Organomet. Chem.* **1974**, *33*, 103.

(43) Bridgeman, A. J.; Mays, M. J.; Woods, A. D. *Organometallics*, in press.

group. It thus exerts less steric pressure and can approach the metal atoms more closely.

The substitution of the $Fe(CO)_3$ group in **8** by the larger $Ru(CO)_3$ group in **9** leads to a widening of the M−Mo−Mo bond angles [Ru(1)−Mo(1)−Mo(2) 58.28(2)°, Ru(1)−Mo(2)−Mo(1) 57.45(2)°, Fe(1)−Mo(1)−Mo(2) 57.49(1)°, Fe(1)−Mo(2)−Mo(1) 56.67(1)°] and a tightening of the Mo−M−Mo bond angle from 65.84(1)° in **8** to 64.26(2)° in **9**. This is to be expected given the longer Ru−Mo bond length (average 2.9823(8) Å) compared to the average Fe−Mo separation of 2.9083(8) Å. The Ru−Mo separations are significantly longer than the distances of 2.8989(9) and 2.9129(8) Å reported for the sulfur-capped complex $[Cp_2(OC)_7Mo_2Ru(\mu_3\text{-}S)]$,[44] but are comparable to the distance of 3.031(1) Å reported in $[Cp_2(OC)_2Mo_2Ru(\mu_3\text{-}S)\{\mu\text{-}\eta^3\text{-}PhCC(H)CPh\}\{\mu_3\text{-}\eta^3\text{-}HC\text{-}C(Ph)CH\}]$.[45]

In both **8** and **9** the Mo(2)−M separation is 0.03 Å longer than the Mo(1)−M separation, reflecting the fact that in each case Mo(1) possesses a semibridging carbonyl group with C(2)−M separations of 2.801 and 2.802 Å for **8** and **9**, respectively. In addition there is some interaction between C(1) and Mo(2) in each complex with C(1)−Mo(2) separations of 2.977 and 2.988 Å, respectively. The Ru−P separation of 2.260(1) Å is consistent with values recorded for other phosphinidine-capped Ru clusters.[46−48]

The ^{31}P NMR spectrum of **8** consists of a singlet at 392.37 ppm, and that of **9** consists of a singlet at 349.63 ppm, which are typical of μ_3-phosphinidene resonances.[49,50]

Crystals of **10** suitable for a single-crystal X-ray diffraction study were grown by slow diffusion of hexane into a dichloromethane solution of **10** under a nitrogen atmosphere at 0 °C. The molecular structure of **10** is shown in Figure 8, and relevant bond lengths (Å) and angles (deg) are included in Table 5.

Complex **10** is perhaps best viewed as a distorted Co_2Mo_2P trigonal bipyramid with two edges bridged by CO groups and a third edge bridged by a CHMe group. The tetrahedral metal core is electron precise, with each metal atom fulfilling the 18-electron rule, and the tetrahedron having the expected electron count of 60. Within the phosphaalkene fragment, the methyl group lies *cis* to the phenyl, as highlighted by the torsion angle C(24)−P(1)−C(25)−C(26) of −48.6°. The P(1)−C(25) vector is at 147.4° to the Mo(1)−Mo(2) vector, compared to corresponding angles of 133.1° and 126.8° in **1a** and **1b**.

The Mo(1)−C(25) separation of 2.280(4) Å is significantly shorter than the corresponding separations in **1a** and **1b** of 2.382(7) and 2.392(3) Å, respectively, although it does fall within the range of Mo−C single bond lengths. In contrast, the P−Mo(1) separation is very long, the value of 2.787(1) Å being far greater than the sum of the covalent radii of Mo and P (2.460 Å), and well outside the range of singly bonded Mo−P separations [range 2.40−2.602(3)].[51] This can be rationalized in part by viewing the bonding as involving η^2 coordination of the P=C π system rather than σ-bonding of both the P and C to the Mo atom.

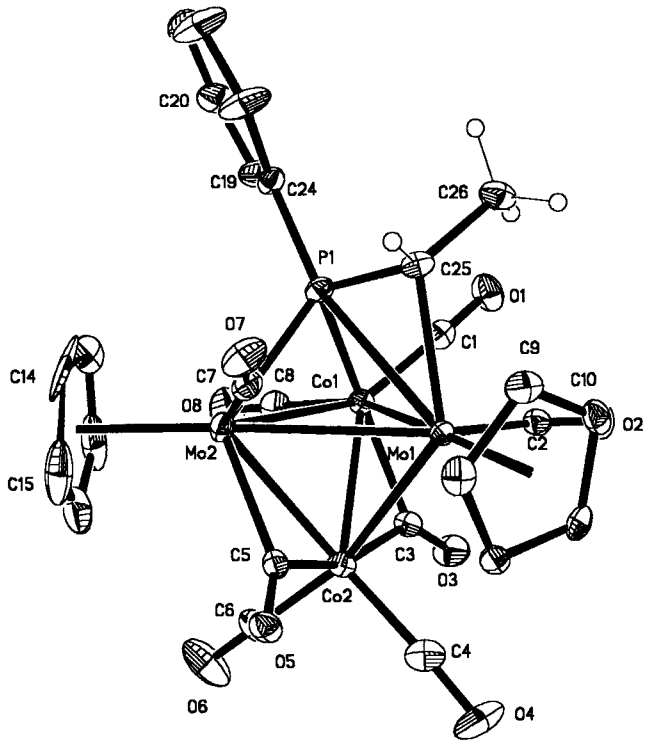

Figure 8. Molecular structure of $[Cp_2(OC)_6Mo_2Co_2(\mu\text{-}CO)_2\{\mu_3\text{-}P(Ph)=C(H)Me\}]$ (**10**) (ring hydrogens omitted for clarity, ORTEP at 50% probability).

The phosphorus atom is in a formal +5 oxidation state and, ignoring the P−Mo(1) bond, can be viewed as being in a distorted tetrahedral environment. The P(1)−C(25) bond length of 1.769(4) Å is somewhat longer than the corresponding bond length in **1a** and **1b**, but is still indicative of a degree of multiple bonding and is comparable to the P−C bond lengths of 1.76(1) and 1.79(1) Å found by Huttner[52] and Stelzer[53] in other μ_3-phosphaalkenes. By way of contrast, the P(1)−C(24) single bond length is 1.832(4) Å.

The Co_2Mo_2 core is, as expected, a distorted tetrahedron. The Co(2)−Mo bond lengths are both shorter than the Co(1)−Mo bond lengths [Co(1)−Mo(1) 2.7474(7) Å, Co(1)−Mo(2) 2.7713(6) Å; Co(2)−Mo(1) 2.7367(6) Å, Co(2)−Mo(2) 2.7104(7) Å], which presumably results from each of the Co(2)−Mo edges being bridged by a carbonyl group. All these values fall well within the range of previously reported Mo−Co bond lengths in Co_2Mo_2 tetrahedra [2.695−2.900(3) Å].[54−57] The Mo−

(44) Adams, R. D.; Babin, J. E.; Tasi, M. *Organometallics* **1988**, *7*, 219.
(45) Adams, R. D.; Babin, J. E.; Tasi, M. *Organometallics* **1987**, *6*, 2247.
(46) Bianchi, M.; Frediani, P.; Faggi, C.; Ianelli, S.; Nardelli, M.; Papaleo, S.; Piccenti, F.; Salvin, A. *J. Organomet. Chem.* **1997**, *536*, 123.
(47) Deeming, A. J.; Doherty, S.; Powell, N. I. *Inorg. Chim. Acta* **1992**, *198*, 469.
(48) Chi, Y.; Lee, G.-H.; Lin, R.-C.; Peng, S.-M. *Inorg. Chem.* **1992**, *31*, 381.
(49) Huttner, G.; Natarajan, K.; Scheidsteger, O. *J. Organomet. Chem.* **1981**, *221*, 301.
(50) Huttner, G.; Mohr, G.; Schneider, J.; v. Seyerl, J. *J. Organomet. Chem.* **1980**, *191*, 161.
(51) Barre, C.; Kubicki, M. M.; Leblanc, J.-C.; Moïse, C. *Inorg. Chem.* **1990**, *29*, 5244 and references therein.
(52) Huttner, G.; Knoll, K.; Wasiucionek, M.; Zsolani, L. *Angew. Chem., Int. Ed. Engl.* **1984**, *23*, 739.
(53) Brauer, D. J.; Ciccu, A.; Fischer, J.; Hessler, G.; Stelzer, O.; Sheldrick, W. S. *J. Organomet. Chem.* **1992**, *428*, 199.
(54) Davis, R. E.; Kashyap, R. P.; Kerby, M. C.; Kyba, E. P.; Mountzouris, J. A. *Organometallics* **1989**, *8*, 852.

Table 5. Selected Bond Lengths (Å) and Angles (deg) for 10

Mo(1)−Mo(2)	3.0149(5)	Mo(1)−Co(1)−Mo(2)	66.23(2)	Mo(2)−Mo(1)−C(25)	80.6(1)
Mo(1)−Co(1)	2.7474(7)	Mo(1)−Co(1)−Co(2)	62.70(2)	Mo(2)−Co(1)−Co(2)	61.67(2)
Mo(1)−Co(2)	2.7367(6)	Mo(1)−Co(1)−P(1)	67.70(3)	Mo(2)−Co(1)−P(1)	55.65(3)
Mo(1)−P(1)	2.787(1)	Mo(1)−Mo(2)−Co(2)	56.81(2)	Mo(2)−P(1)−C(25)	113.1(1)
Mo(1)−C(25)	2.280(4)	Mo(1)−Mo(2)−Co(1)	56.51(2)	Mo(2)−P(1)−C(24)	123.9(1)
Mo(2)−Co(1)	2.7713(6)	Mo(1)−Mo(2)−P(1)	60.94(3)	Mo(2)−C(7)−O(7)	168.1(4)
Mo(2)−Co(2)	2.7104(7)	Mo(1)−Co(2)−Mo(2)	67.21(2)	Co(1)−Mo(1)−Co(2)	54.16(2)
Mo(2)−P(1)	2.371(1)	Mo(1)−Co(2)−Co(1)	63.14(2)	Co(1)−Mo(1)−P(1)	46.51(2)
Co(1)−Co(2)	2.4966(8)	Mo(1)−P(1)−C(24)	164.9(1)	Co(1)−Mo(2)−Co(2)	54.17(2)
Co(1)−P(1)	2.185(1)	Mo(1)−P(1)−C(25)	54.7(1)	Co(1)−Mo(2)−P(1)	49.55(3)
P(1)−C(25)	1.769(4)	Mo(1)−C(2)−O(2)	169.4(4)	Co(1)−P(1)−C(24)	117.7(1)
P(1)−C(24)	1.832(4)	Mo(1)−C(25)−P(1)	86.0(2)	Co(1)−P(1)−C(25)	109.4(1)
		Mo(1)−C(25)−C(26)	120.5(3)	Co(2)−Mo(2)−P(1)	98.58(3)
		Mo(2)−Mo(1)−Co(1)	57.27(1)	C(24)−P(1)−C(25)	112.3(2)
		Mo(2)−Mo(1)−Co(2)	55.98(2)	C(26)−C(25)−P(1)	117.9(3)
		Mo(2)−Mo(1)−P(1)	48.04(2)	C(25)−Mo(1)−Co(2)	127.9(1)

Mo separation of 3.0149(5) Å is somewhat greater than that in most Mo_2Co_2 tetrahedra, but is slightly shorter than the value of 3.024(1) Å recorded for the unsubstituted complex $[Cp_2(OC)_7Mo_2Co_2(\mu\text{-}CO)_3]$.[57] The terminal CO group on each Mo is actually semibridging [O(7)−C(7)−Mo(2) 168.1(4)°, O(2)−C(2)−Mo(1) 169.4(4)°] with calculated separations of 2.941 Å [C(7)−Mo(1)] and 2.697 Å [C(2)−Co(1)].

The ^{31}P NMR spectrum of **10** consists of a singlet at 43.86 ppm, which is significantly upfield from that of **1**. Comparisons of the chemical shift may be made to other cluster-stabilized phosphaalkenes of type V (Figure 1), the resonance of **10** being significantly upfield from these values, which are in the range 220−260 ppm, although all of these other complexes contain a phosphaalkene coordinated to a group VIII metal triangle.[51] The ^1H NMR spectrum consists of a multiplet at 7.50−7.46 ppm which is assigned to the phenyl group. Two distinct cyclopentadienyl resonances are observed at 5.01 and 4.80 ppm. A broad singlet at 1.52 ppm is assigned to the P═C*H* proton, and a double doublet at 1.34 ppm ($^3J_{P-H}$ = 19.05 Hz, $^3J_{H-H}$ = 6.60 Hz) is assigned to the P═C*Me* group.

The IR spectrum contains absorptions at 2073, 2030, 2012, and 1999 cm^{-1}, clearly showing that $Co(CO)_2$ fragments have been introduced. An additional absorption at 1829 cm^{-1} confirms the presence of a bridging carbonyl group.

DFT Studies of *cis/trans*-[$Cp_2(OC)_4Mo_2$\{μ-η^1:η^2-P(Ph)═C(H)Me\}]. Due to the paucity of complexes such as **1a** and **1b** it was decided to undertake a thorough analysis of these two isomers to describe their bonding more fully.

The DFT study reveals that *cis*-**1b** is in fact the thermodynamically favored product, being approximately 35 kJ mol^{-1} more stable than *trans*-**1a**. Modeling of the transition state for isomerization, which is assumed to involve breaking of the P═C π-bond so that the p orbitals on the two atoms lie orthogonal to each other, suggests that the activation barrier to isomerization is about 180 kJ mol^{-1}.

In the related metallophosphaalkenes $[Cp_2(OC)_2Fe_2\{\mu\text{-}\eta^1\text{:}\eta^2\text{-P(M)═C(H)SMe}\}]$ (M = $FeCp(CO)_2$) Weber[5] proposed three canonical forms which could be used to describe the bonding in such complexes, and these are shown in Figure 9.

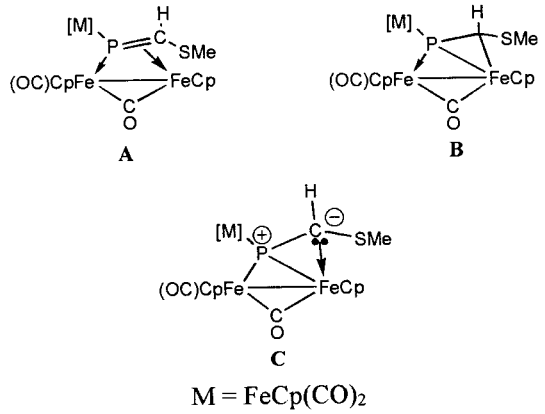

Figure 9. Proposed canonical forms of $[Cp_2(OC)_2Fe_2\{\mu\text{-}\eta^1\text{:}\eta^2\text{-P(M)═C(H)SMe}\}]$.

Table 6. Calculated Bond Orders and Charge Densities for 1a and 1b

	1a	1b		1a	1b
P(1)−C(21)	0.90	0.95	Mo(1)	−0.28	−0.30
P(1)−Mo(1)	0.88	0.84	Mo(2)	−0.05	−0.04
P(1)−Mo(2)	0.69	0.73	P(1)	+0.45	+0.44
Mo(1)−Mo(2)	0.42	0.41	C(21)	−0.67	−0.64
C(21)−Mo(2)	0.65	0.65	H(21)	−0.36	+0.38
Mo(2)−C(4)	1.25	1.21			
Mo(1)−C(4)	0.17	0.18			

The DFT analysis suggests that form B most accurately describes the bonding, as can be seen by inspecting the P−C bond orders (Table 6), which are indicative only of a single bond interaction. The bond orders of 0.90 and 0.95 found in **1a** and **1b** may be compared to a bond order of 1.88 which was calculated for the P═C bond in the free phosphaalkene *cis*-P(Ph)═C(Me)H. Furthermore, the Mo(1)−P and Mo(2)−C(21) bond orders are both consistent with a single bond formulation. An examination of the HOMOs reveals that they are derived from interaction of the P═C π^* orbital (Figure 10) with an antibonding orbital of the $Cp_2Mo_2(CO)_4$ fragment, reducing the P−C bond order between P(1) and C(21).

As noted in our preliminary communiation the molecular structures of **1a** and **1b** both contain a semibridging carbonyl group between Mo(1) and C(4);[6] this is highlighted by the DFT results, which show Mo(1)−C(4) bond orders of 0.17 and 0.18 for **1a** and **1b**, respectively. The analysis also reveals that Mo(1) has a good deal of negative charge buildup, with a charge of −0.28 and

(55) Kaganovich, V. S.; Mironov, A. V.; Rybinskaya, M. I.; Stovokhotov, Y. L.; Struchkov, Y. T. *J. Organomet. Chem.* **1989**, *372*, 339.
(56) Curtis, M. D.; Haggerty, B. S.; Rheingold, A. L.; Riaz, U. *Organometallics* **1990**, *9*, 2647.
(57) Curnow, O. J.; Curtis, M. D.; Haggerty, B. S.; Kanf, J. W.; Rheingold, A. L.; Riaz, U. *Organometallics* **1995**, *14*, 5337.

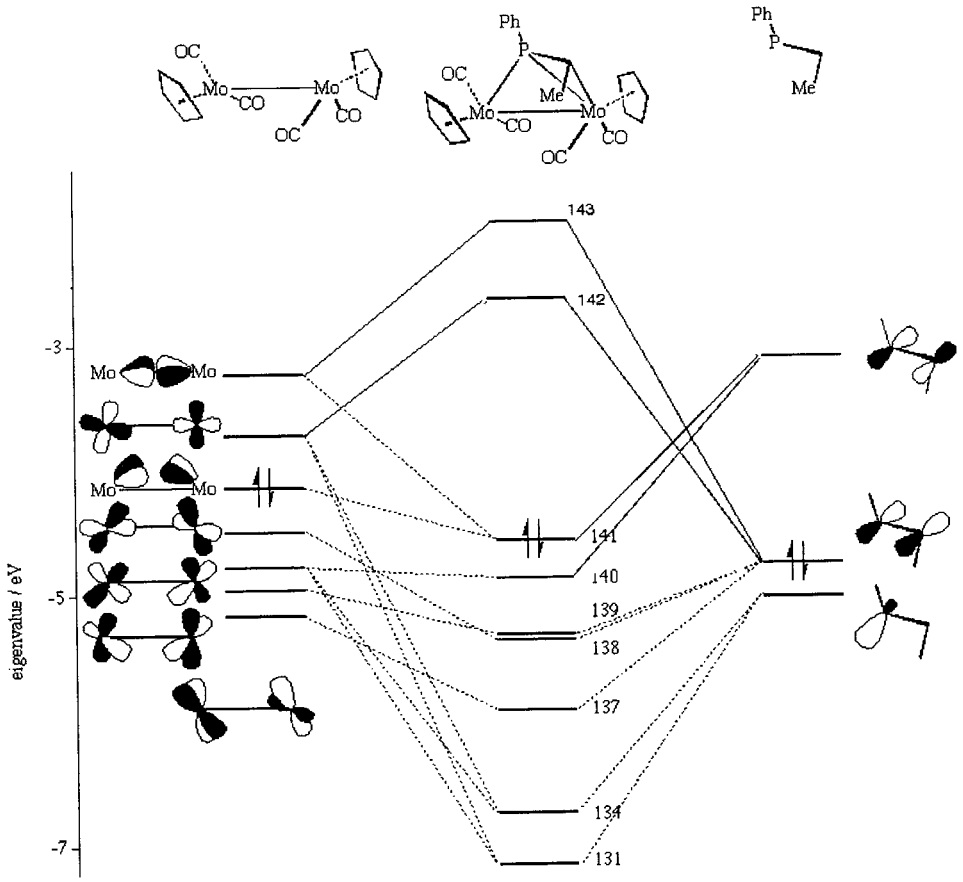

Figure 10. Molecular orbital diagram of **1a**.

−0.30 in **1a** and **1b**, respectively; presumably the semibridging carbonyl is formed to help remove excess electron density from this center.

There is little difference between the molecular orbital diagrams of **1a** and **1b**, so for simplicity's sake only the MO diagram of **1a** is shown (Figure 10). The major difference between the two stems from the relative energies of the orbitals in **1a** and **1b**, the HOMO being more stabilized in **1b** than **1a**. Furthermore, the energies of the two LUMOs (orbitals 142 and 143) are −2.709 and −2.113 eV for **1a** and −2.562 eV and −2.080 eV for **1b**, thus indicating that the HOMO−LUMO separation is larger for **1b** than it is for **1a**. Orbital 142 corresponds to the Mo−Mo σ^*, which is the LUMO of the Mo_2 fragment, interacting with the P−C π orbital. Orbital 143 corresponds to the Mo−Mo π^* interacting with the P−C π orbital.

The molecular orbital diagram clearly indicates that the HOMO is antibonding with respect to both the metal−metal bond and the P═C π-bond. The fact that both the P═C π and π^* orbitals are involved in bonding contributions suggests that there is no net π-bonding, as confirmed by the calculated bond orders (the free phosphaalkeene has a P═C bond order of 1.86). Additionally, as can be seen from inspection of MOs 140−143, these orbitals contain a significant contribution from the CO groups, suggesting that these groups should be labile on photolysis.

Experimental Section

Unless otherwise stated all experiments were carried out under an atmosphere of dry, oxygen-free nitrogen, using conventional Schlenk line techniques, and solvents freshly distilled from the appropriate drying agent. NMR spectra were recorded in $CDCl_3$ using a Bruker DRX 400 spectrometer, with TMS as an external standard for ^1H and ^{13}C spectra and 85% aqueous H_3PO_4 as an external standard for ^{31}P spectra. Infrared spectra were, unless otherwise stated, recorded in dichloromethane solution in 0.5 mm NaCl solution cells, using a Perkin-Elmer 1710 Fourier transform spectrometer. FAB mass spectra were obtained using a Kratos MS 890 instrument, using 3-nitrobenzyl alcohol as a matrix. Preparative TLC was carried out on 1 mm silica plates prepared at the University of Cambridge. Column chromatography was performed on Kieselgel 60 (70−230 mesh ASTM). Unless otherwise stated, all reagents were obtained from commercial suppliers and used without further purification. [$Cp_2(OC)_4Mo_2$-(μ-η^1:η^2-PhP═CHMe)] was prepared by the literature method.[6]

Crystal Structure Determinations. X-ray diffraction data were collected using a Nonius-Kappa CCD diffractometer, equipped with an Oxford Cryostream cryostream. Data reduction and cell refinement were performed with the programs DENZO[58] and COLLECT,[59] and multiscan absorption corrections were applied to all intensity data with the program SORTAV.[60] Structures were solved and refined with the programs SHELXS97 and SHELXL97,[61] respectively.

Atomic coordinates, bond lengths and angles, and thermal parameters have been deposited in the Cambridge Crystallographic Data Centre (CCDC). Any request to the CCDC for this material should quote the full literature citation.

Computational Details. All DF calculations were performed using the DeFT code written by St-Amant in the linear

(58) Otwinowski, Z.; Minor, W. *Methods Enzymol.* **1997**, *276*, 307.
(59) Hooft, R. COLLECT, Nonius BV, Delft, The Netherlands, 1998.
(60) Blessing, R. H. *Acta Crystallogr.* **1995**, *A51*, 33.
(61) Sheldrick, G. M. SHELXS97 and SHELXL97, University of Göttingen, Germany.

combination of Gaussian-type orbitals framework.[62] The calculations used the local spin density (LSD) approximation of the correlation part of the exchange-correlation potential of Vosko et al.[63] with the Becke[64] and Perdew[65] nonlocal corrections for exchange and correlation, respectively. Basis sets of double-ζ quality were used for molybdenum and of triple-ζ quality for all other atoms in all electron treatments. Bond orders were calculated from the density matrix according to the prescription suggested by Mayer.[66] Molecular orbital plots were produced using the Molden program.[67]

Protonation of *cis/trans*-[$Cp_2(OC)_4Mo_2$\{μ-η^1:η^2-P(Ph)=C(H)Me\}] (1). To a solution of **1** (250 mg, 0.44 mmol) in acetonitrile (40 mL) in a vessel open to the air was added 54% HBF_4·Et_2O (0.27 mL, 4 equiv) and the resulting solution stirred for 30 min, during which time the solution color changed from brown to red. The reaction mixture was condensed to 10 mL and Et_2O (25 mL) added to precipitate a red-brown solid. The solid was washed with Et_2O to yield red [{$Cp(MeCN)_4Mo$}$_2$O][BF_4]$_4$ (**2**) (267 mg, 74%). Crystals suitable for an X-ray diffraction study were grown by vapor diffusion of Et_2O into an acetronitrile solution of **2** at 0 °C.

It should be noted that if a high vacuum was applied to the sample, it began to decompose substantially, precluding accurate elemental analysis.

IR (ν(CN)): 2159(m), 2154(m) cm^{-1}. ^1H NMR: δ 6.21 (s, 10H, Cp), 2.47 (s, 24H, CH_3CN). ^{13}C NMR: δ 132.17 (C≡N), 109.77 (Cp), 3.57 (H_3*C*CN). Anal. Calcd for $B_4C_{26}F_{16}H_{34}Mo_2N_8O$: C 30.80, H 3.38, N 11.0. Found: C 29.02, H 3.33, N 9.55.

Reaction of 1 with LiB^{s}Bu$_3$H. A 1 M solution of LiB^{s}Bu$_3$H in THF (0.52 mL, 1 equiv) was added dropwise at −78 °C to a solution of **1** (300 mg, 0.52 mmol) in THF (40 mL). The resulting solution was stirred for 30 min, during which time the solution changed color from brown to purple. Addition of 54% HBF_4·Et_2O caused a color change from purple to orange. The solvent was removed under reduced pressure and the residue redissolved in the minimum amount of CH_2Cl_2. Filtration through a silica pad yielded orange [$Cp_2(OC)_4Mo_2$(μ-PPhEt)(μ-H)] (**3a**) (246 mg, 83%).

Crystals suitable for a single-crystal X-ray diffraction study were grown by slow evaporation of a CH_2Cl_2/hexane solution of **3a** at 0 °C.

IR (ν(CO)): 1959(m), 1940(vs), 1882(s), 1875(s) cm^{-1}. ^1H NMR: δ 7.35−7.00 (m, 5H, Ph), 5.23 (s, br, 5H, Cp), 4.80 (s, br, 5H, Cp), 3.69 (s, vbr, 2H, P−CH_2), 1.40 (d, br, $^2J_{P-H}$ = 17.56 Hz, 3H, P−CH_2CH_3), −11.60 (d, $^2J_{P-H}$ = 37.32 Hz, 1H, μ-H). ^{13}C NMR: δ 224.86 (s, br *C*O), 199.7 (s, br, *C*O), 142.96−128.07 (m, Ph), 91.45 (s, br, Cp), 30.31 (d, $^1J_{P-C}$ = 22.84 Hz, P*C*H$_2$), 12.56 (d, $^2J_{P-C}$ = 4.60 Hz, PCH$_2$*C*H$_3$). ^{31}P NMR: δ 179.61 (s, μ-*P*PhEt). Anal. Calcd for $C_{22}H_{21}Mo_2O_4P$: C 45.84, H 3.55, P 5.38. Found: C 45.72, H 3.75, P 5.50. FAB MS: *m*/*z* 572 (M^+), $M^+ - n$CO (n = 1−4).

The reprotonation was also effected by addition of 20% DCl in D_2O (0.1 mL, 1 equiv) to yield [$Cp_2(OC)_4Mo_2$(μ-PPhEt)(μ-D)] (**3b**).

^2H NMR: δ −14.52 (d, $^2J_{P-D}$ = 5.61 Hz, μ-D). ^{31}P NMR: δ 179.61 (t, $^2J_{P-D}$ = 5.61 Hz, μ-P).

Thermolysis of 1 with Ph_2PH. Thermolysis of a solution of **1** (150 mg, 0.26 mmol) and Ph_2PH (0.1 mL, 2 equiv) in toluene (60 mL) caused a color change from brown to red. The solvent was removed under reduced pressure, and the residue was redissolved in the minimum amount of CH_2Cl_2, applied to the base of TLC plates, and eluted with 1:1 hexane/CH_2Cl_2 to yield a trace of **1** and a trace of red [$Cp_2(OC)(O)Mo_2$(μ-PPh_2)(μ-PPhEt)] as a mixture of *cis*-**6** and *trans*-**5** isomers.

Photolysis of 1 with Ph_2PH. Nitrogen was bubbled through a solution of **1** (150 mg, 0.26 mmol) and Ph_2PH (0.1 mL, 2 equiv) in toluene (80 mL), and the mixture was photolyzed using a 125 W UV lamp for 30 min. The solvent was removed in vacuo and the residue redissolved in the minimum amount of CH_2Cl_2, applied to the base of TLC plates, and eluted with 3:2 CH_2Cl_2/hexane to yield green [$Cp_2(OC)_2$-Mo_2(μ-PPhEt)(μ-PPh_2)] (**4**) (70 mg, 39%).

IR (ν(CO)): 1863 cm^{-1}. ^1H NMR: δ 7.70−7.15 (m, 15H, Ph), 5.39 (s, 5H, Cp), 5.28 (s, 5H, Cp), 3.14 (m, 1H, P−C*H*H), 2.05 (m, 1H, P−CH*H*), 1.31 (dt, $^3J_{P-H}$ = 17.39 Hz, $^3J_{H-H}$ = 7.41 Hz, 3H, P−CH_2–CH_3). ^{31}P NMR: δ 89.10 (d, $^2J_{P-P}$ = 8.8 Hz, μ-*P*Ph_2), 84.92 (d, $^2J_{P-P}$ = 8.8 Hz, μ-*P*PhEt). Anal. Calcd for $C_{32}H_{30}Mo_2O_2P_2$: C 54.88, H 4.31, P 8.84. Found: C 55.16, H 4.38, P. 8.76. FAB MS: *m*/*z* 700 (M^+), M^+ − C.

Oxidation of [$Cp_2(OC)_2Mo_2$(μ-PPhEt)(μ-PPh_2)] (4). A solution of **4** (100 mg, 0.15 mmol) in CH_2Cl_2 was stirred in a sealed, air-filled flask for 4 h, during which time the solution turned brown. The solvent was removed, and the residue was dissolved in the minimum amount of CH_2Cl_2 and applied to the base of TLC plates. Elution with 3:2 CH_2Cl_2/hexane yielded *trans*-[$Cp_2(OC)(O)Mo_2$(μ-PPhEt)(μ-PPh_2)] (**5**) (34 mg, 28%) and *cis*-[$Cp_2(OC)(O)Mo_2$(μ-PPhH)(μ-PPh_2)] (**6**) (7 mg, 6%).

Data Assigned to 5. IR (ν(CO)): 1847 cm^{-1}. ^1H NMR: δ 8.20−7.05 (m, 15H, Ph), 5.24 (s, 5H, Cp), 4.98 (s, 5H, Cp), 3.16−3.10 (m, PC*H*H), 2.10−2.00 (m, PCH*H*), 1.69−1.61 (m, PCH$_2$CH_3). ^{31}P NMR: δ 169.86 (d, $^2J_{P-P}$ = 6.55 Hz, μ-*P*Ph_2), 154.7 (d, $^2J_{P-P}$ = 6.55 Hz, μ-*P*PhEt). Anal. Calcd for $C_{31}H_{30}$-$Mo_2O_2P_2$: C 54.08, H 4.39, P 9.00. Found: C 54.61, H 4.54, P 9.16. FAB MS *m*/*z* 691 (M^+), M^+ − CO.

Data Assigned to 6. IR (ν(CO)): 1831 cm^{-1}. ^1H NMR: δ 8.20−7.05 (m, 15H, Ph), 4.82 (s, 5H, Cp), 4.80 (s, 5H, Cp), 3.16−3.10 (m, PC*H*H), 2.10−2.00 (m, PCH*H*), 1.69−1.61 (m, PCH$_2$CH_3). ^{31}P NMR: δ 169.43 (d, $^2J_{P-P}$ = 5.5 Hz, μ-*P*Ph_2), 168.96 (d, $^2J_{P-P}$ = 5.5 Hz, μ-*P*PhEt). FAB MS *m*/*z* 691 (M^+), M^+ − CO.

Photolysis of 1 with PhC≡CH. Nitrogen was bubbled through a solution of **1** (300 mg, 0.52 mmol) and PhC≡CH (0.16 mL, 3 equiv) in toluene (200 mL), and the mixture was photolyzed using a 400 W UV lamp for 1 h. The solvent was removed in vacuo and the residue redissolved in the minimum amount of CH_2Cl_2, applied to the base of TLC plates, and eluted with 3:2 CH_2Cl_2/hexane to yield orange [$Cp_2(OC)_4Mo_2$-{μ-PhP(C(Me)HC(H)=CPh}] (**7**) (160 mg, 46%).

Crystals suitable for a single-crystal X-ray diffraction study were grown by slow evaporation of a CH_2Cl_2/hexane solution of **7** at −15 °C.

IR (ν(CO)): 2002(w), 1985(vs), 1978(s,sh), 1936(s), 1892(m), 1867(m) cm^{-1}. ^1H NMR: δ

(*S* isomer) 7.58−7.10 (m, 10H, Ph), 5.86 (dd, $^3J_{P-H}$ = 43.04 Hz, $^3J_{H-H}$ = 3.91 Hz, 1H, C=CH), 5.13 (s, 5H, Cp), 4.88 (s, 5H, Cp), 3.90 (m, br, 1H, P−C*H*), 1.64 (dd, $^3J_{P-H}$ = 15.65 Hz, $^3J_{H-H}$ = 7.83 Hz, 3H, P−C−CH_3);

(R isomer) 7.58−7.10 (m, 10H, Ph), 5.88 (d, br, $^2J_{P-H}$ = 36.19 Hz, 1H, C=CH), 5.30 (s, 5H, Cp), 4.98 (s, 5H, Cp), 3.60 (m, br, 1H, P−C*H*), 1.05 (dd, $^3J_{P-H}$ = 13.69 Hz, $^3J_{H-H}$ = 6.85 Hz, 3H, P−C−CH_3).

^{31}P NMR: δ 226 (s, vbr, μ-Ph*P*). Anal. Calcd for $C_{30}H_{25}$-Mo_2O_4P: C 53.59, H 3.75, P 4.61. Found: C 53.06, H 3.70, P 4.66. FAB MS *m*/*z* 673 (M^+), $M^+ - n$CO (n = 1, 2), M^+ − C (sample oxidized).

Photolysis of 1 with $Fe(CO)_5$. Nitrogen was bubbled through a solution of **1** (150 mg, 0.26 mmol) and $Fe(CO)_5$ (0.07 mL, 2 equiv) in toluene (80 mL), and the mixture was photolyzed using a 125 W UV lamp for 30 min. The solvent was removed in vacuo and the residue redissolved in the minimum amount of CH_2Cl_2, applied to the base of TLC plates, and eluted with 1:1 hexane/CH_2Cl_2 to yield a trace of **1** and [$Cp_2(OC)_7Mo_2Fe$(μ_3-PPh)] (**8**) (90 mg, 50%).

(62) St-Amant, A. DeFT, A FORTRAN program, University of Ottawa, Canada, 1994.
(63) Vosko, S. H.; Wilk L.; Nusair, M. *Can. J. Phys.* **1980**, *58*, 1200.
(64) Becke, A. D. *Phys. Rev. A* **1988**, *38*, 3098.
(65) Perdew, J. D. *Phys. Rev. B* **1986**, *33*, 8822.
(66) (a) Mayer, I. *Chem. Phys. Lett.* **1983**, *97*, 270. (b) Mayer, I. *Int. J. Quantum Chem.* **1984**, *26*, 151.
(67) Schaftenaar G.; Noordik, J. H. Molden: a pre- and post-processing program for molecular and electronic structures. *J. Comput.-Aided Mol. Des.* **2000**, *14*, 123.

Crystals suitable for a single-crystal X-ray diffraction study were grown by slow diffusion of hexane into a CH_2Cl_2 solution of **8** at −15 °C.

IR (ν(CO)): 2069(m), 2012(m), 1996(s), 1988(s,sh), 1938(m), 1874(w) cm^{-1}. ^1H NMR: δ 7.57−7.38 (m, 5H, Ph), 5.14 (s, 5H, Cp). ^{31}P NMR: δ 392.37 (s, μ_3-*P*Ph). Anal. Calcd for $C_{23}FeH_{15}Mo_2O_7P$: C 40.50, H 2.21, P 4.54. Found: C 40.32, H 2.19, P 4.52. FAB MS *m*/*z* 682 (M^+), $M^+ - n$CO (n = 1−5).

Thermolysis of 1 with $Ru_3(CO)_{12}$. A solution of **1** (150 mg, 0.26 mmol) and $Ru_3(CO)_{12}$ (180 mg, 1 equiv) in toluene (50 mL) was refluxed for 3 h. The solvent was removed in vacuo and the residue redissolved in the minimum amount of CH_2Cl_2, applied to the base of TLC plates, and eluted with 1:1 hexane/CH_2Cl_2 to give *trans*-[$Cp_2(OC)_4Mo_2\{\mu$-η^1:η^2-P(Ph)═C(H)Me}] (**1a**) (9 mg, 6%), *cis*-[$Cp_2(OC)_4Mo_2\{\mu$-η^1:η^2-P(Ph)═C(H)Me)] (**1b**) (27 mg, 18%), and [$Cp_2(OC)_7Mo_2Ru(\mu_3$-PPh)] (**9**) (66 mg, 35%) as well as several other trace bands and a decomposition product.

Crystals suitable for a single-crystal X-ray diffraction study were grown by slow diffusion of hexane into a CH_2Cl_2 solution of **9** at −15 °C.

IR (ν(CO)): 2037(vs), 2026(s), 2002(m), 1954(m), 1845(s), 1826(s) cm^{-1}. ^1H NMR: δ 7.84−7.42 (m, 5H, Ph), 5.08 (s, 5H, Cp). ^{31}P NMR: δ 349.63 (s, μ_3-*P*Ph). Anal. Calcd for $C_{23}H_{15}Mo_2O_7PRu$: C 37.98, H 2.08, P 4.26. Found: C 38.03, H 2.10, P 4.26. FAB MS *m*/*z* 727(M^+), $M^+ - n$CO (n = 1−4).

Thermolysis of 1 with $Co_2(CO)_8$. A solution of [$Cp_2(OC)_4Mo_2\{\mu$-η^1:η^2-P(Ph)═C(H)Me}] (300 mg, 0.52 mmol) and $Co_2(CO)_8$ (300 mg, 2 equiv) in heptane (70 mL) was refluxed for 3 h. The solvent was removed under reduced pressure and the residue redissolved in the minimum amount of CH_2Cl_2, applied to the base of TLC plates, and eluted with 1:1 hexane/CH_2Cl_2 to yield a trace of **1** and [$Cp_2(OC)_6Mo_2Co_2(\mu$-CO)$_2\{\mu_3$-P(Ph)═C(H)Me}] (**10**) (83 mg, 20%).

Crystals suitable for a single-crystal X-ray diffraction study were grown by slow diffusion of hexane into a CH_2Cl_2 solution of **10** at −15 °C.

IR (ν(CO)): 2073(m), 2030(vs), 2012(s), 1999(m), 1926(s), 1879(m), 1829(w) cm^{-1}. ^1H NMR: δ 7.50−7.46 (m, 5H, Ph), 5.01 (s, 5H, Cp), 4.80 (s, 5H, Cp), 1.52 (s, br, 1H, P═CH) 1.34 (dd, $^3J_{P-H}$ = 19.05 Hz, $^3J_{H-H}$ = 6.60 Hz, 3H, P═CCH_3). ^{31}P NMR: δ 43.86 (s, μ_3-Ph*P*═CHMe). Anal. Calcd for $C_{26}Co_2H_{19}Mo_2O_8P$: C 38.93, H 2.64, P 5.28. Found: C 38.93, H 2.49, P 3.86. FAB MS *m*/*z* 800 (M^+), $M^+ - n$CO (n = 1−8).

Acknowledgment. We are grateful to the EPSRC for a Quota award to A.D.W. and for financial support toward the purchase of the diffractometer, and to ICI for a CASE award to A.D.W. We thank Dr. J. E. Davies for measuring the diffraction data, and for help with the X-ray structure solutions.

Supporting Information Available: Tables giving the crystal data and structure refinement, equivalent atomic coordinates and isotropic displacement parameters, bond lengths and angles, anisotropic displacement parameters, and hydrogen coordinates and isotropic displacement parameters for **2**, **4**, and **7**−**10**. This material is available free of charge via the Internet at http://pubs.acs.org.

OM001089K